13. Radiation*

13.1 Introduction

The radiation calculation scheme adopted in the MRI•GCM-I closely follows the one described in Arakawa and Mintz (1974).

The solar radiation incident on the top of the model atmosphere has both seasonal and diurnal variations. In the MRI•GCM-I, the solar flux under cloudless conditions is depleted by ozone absoption, water vapor absorption and Rayleigh scatterring. The model forms interactive clouds, such as clouds by large scale condensation and cirrus. They influence the radiational heating fields strongly by absorption and reflection. The albedo of the earth's surface is determined diagnostically by the model as a simple function of surface conditions.

The parameterization of the solar radiation is based on Katayama (1972). The solar radiation is divided into two parts at the wave length $\lambda = \lambda_c = 0.9\mu$.

i) The part $\lambda < \lambda_c$ is called "scattered" part. Rayleigh scattering is considered in this wave length region below 200 mb.

ii) The part $\lambda > \lambda_c$ is called "absorbed" part, where absorption by water vapor is considered, while Rayleigh scattering is neglected.

For the long wave radiation, we adopt a hybrid scheme proposed by Schlesinger (1976) ; the scheme consists of two different methods which are connected with each other at 30 km level.

i) From the surface up to the 30 km level, we use the method developed by Katayama (1972) ; weighted mean transmission functions defined for the entire band are used to calculate long wave radiation flux and its flux divergence. Water vapor, carbon dioxide and ozone are treated as absorbers.

ii) Above the 30 km level, we adopt the long wave radiative cooling parameterization developed by Dickinson (1973).

Usually radiation model is a time-consuming part of the GCM. This is one of the reasons for neglecting diurnal variations in the radiative flux calculation in many GCMs. It is pointed out that diurnal variations are taken account of in the current radiation model, which is realized by an adoption of an economical scheme for long wave radiation developed by

---

* This chapter is prepared by I. Yagai.

Katayama (1972). Therefore various prognostic variables especially those associated with the planetary boundary layer undergo their diurnal variations.

13.2 Terrestrial radiation

13.2.1 Basic equations

The upward and the downward fluxes of terrestrial radiation, $R_z^{\uparrow}$, and $R_z^{\downarrow}$, are given by ;

$$R_z^{\uparrow} = \int_0^{\infty} \pi B_\nu(T_z) d\nu + \int_0^{\infty} d\nu \int_{T_z}^{T_g} \pi \frac{dB_\nu(T)}{dT} \tau_f\{\ell_\nu(u_z - u)\} dT \tag{13.1}$$

$$R_z^{\downarrow} = \int_0^{\infty} \pi B_\nu(T_z) d\nu + \int_0^{\infty} d\nu \int_{T_z}^{T_T} \pi \frac{dB_\nu(T)}{dt} \tau_f\{\ell_\nu(u - u_z)\} dT$$

$$- \int_0^{\infty} \pi B_\nu(T_T) \tau_f\{\ell_\nu(u_\infty - u_z)\} d\nu \tag{13.2}$$

where $u_z = u(T_z)$ is the effective amount of absorbing medium (water vapor, carbon dioxide and ozone) in the vertical air column from the earth's surface to the level z, T_z the temperature at level z, T_g the ground temperature, B_ν the Plank's radiation function expressed in terms of frequency ν, ℓ_ν the absorption coefficient, τ_f the transmission function of a slab at frequency ν, T_T the temperature of the effective lid of the atmosphere. In the 12 layer version of the MRI•GCM-I, the long wave flux is calculated up to the 10 mb level, therefore T_T is defined as the vertical mean temperature above 10 mb. As for the tropospheric version of the MRI•GCM-I, T_T is assigned the value shown in Fig. 13.1 based on the annually averaged temperature in the lower stratosphere.

The net upward flux R_z is defined as

$$R_z = R_z^{\uparrow} - R_z^{\downarrow} \tag{13.3}$$

The heating rate is given by

$$\left(\frac{\partial T}{\partial t}\right)_{tr} = \frac{g}{c_p} \frac{\partial R_z}{\partial p} \tag{13.4}$$

where g is the acceleration due to gravity and c_p is the specific heat of air at constant pressure.

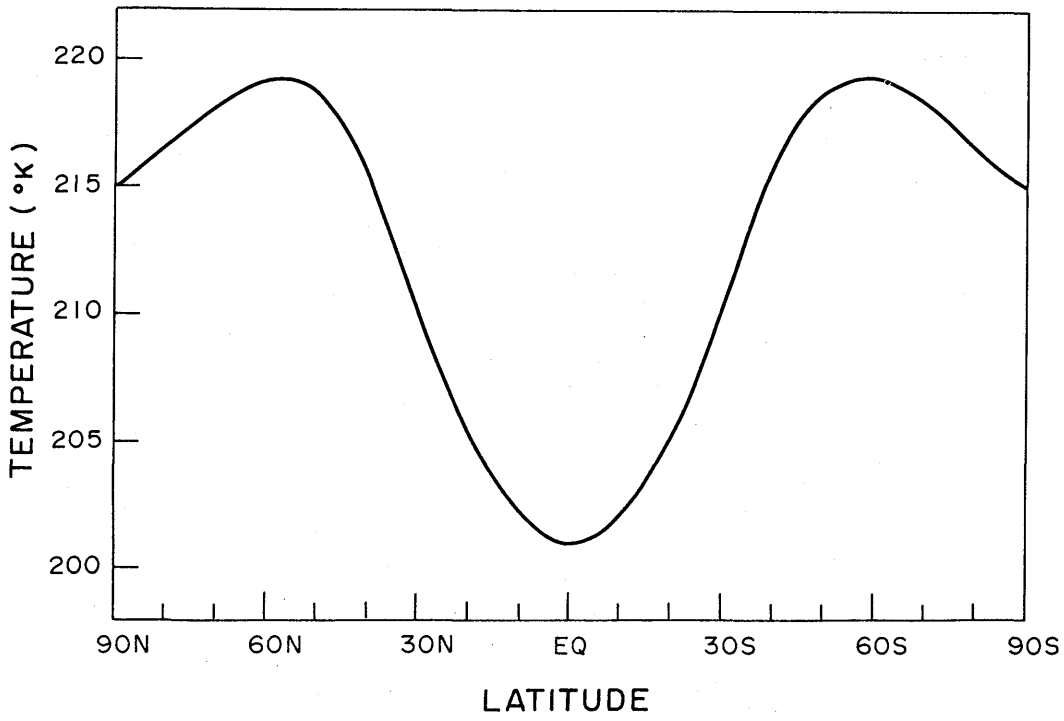

Fig. 13.1 Latitudinal variation of T_T, the temperature of the effective lid adopted in the troposheric version of the MRI • GCM-I. T_T is based on the annually averaged temperature in the lower stratosphere.

13.2.2 Simplification : Weighted mean transmission functions

In order to simplify the computation of equations (13.1) and (13.2), Yamamoto (1952) introduced the following weighted mean transmission functions.

$$\tau(u^*,T)\equiv\left[\pi\frac{dB(T)}{dT}\right]^{-1}\int_0^\infty \pi\frac{dB_\nu(T)}{dT}\tau_f\{\ell_{\nu,o}\, u^*\}d\nu \tag{13.5}$$

and

$$\tilde{\tau}(u^*,T)\equiv\{\pi B(T)\}^{-1}\int_0^\infty \pi B_\nu(T)\tau_f\{\ell_{\nu,o}\, u^*\}d\nu \tag{13.6}$$

where

$$\pi B(T)=\int_0^\infty \pi B_\nu(T)d\nu=\sigma T^4$$

$$\ell_{\nu,o}u^*=\ell_\nu u$$

and σ is the Stefan - Boltzman constant, $\ell_{\nu,o}$ the absorption coefficient at the standard

pressure p_o. The effective absorber amount u^* is given by

$$u^*_n(p)=\frac{1}{g}\int_p^{Ps} q_n(p')\left(\frac{p'}{p_o}\right)^{\alpha_n}dp' \tag{13.7}$$

where p_s is the surface pressure, q_n the absorber mixing ratio, and n a symbol of either H_2O, CO_2, or O_3. Pressure scaling factor α_n is given in Table 13.1.

Yamamoto found for water vapor that the dependence of $\tau(u^*, T)$ on temperature is weak in between 210°K and 320°K. Furthermore, according to Schlesinger (1976), the temperature dependence of τ on carbon dioxide and ozone is weak in between 190°K and 310°K. Therefore, we introduce the following approximation

$$\tau(u^*, T)\fallingdotseq\tau(u^*,\bar{T}) \qquad \text{for } T\geq T_c=220°K \tag{13.8}$$

where $\bar{T}=260°K$.

With the use of (13.8), equations (13.1) and (13.2) are transformed into the following form

$$R_z^{\downarrow}=\pi B_z-\pi B_c\tilde{\tau}(u^*_\infty-u^*_z,T_c)-(\pi B_T-\pi B_c)\tau(u^*_\infty-u^*_z,\bar{T})$$

$$+\int_{\pi B_z}^{\pi B_T}\tau(u^*-u^*_z,\ \bar{T})d(\pi B) \tag{13.9}$$

and

$$R_z^{\uparrow}=\pi B_z+\int_{\pi B_z}^{\pi B_s}\tau(u^*_z-u^*,\ \bar{T})d(\pi B) \tag{13.10}$$

where $B_z=B(T_z)$, $B_c=B(T_c)$, $B_T=B(T_T)$. Following Yamamoto (1952), the transmission functions of a mixture of water vapor, carbon dioxide, and ozone may be approximated by the product of their respective transmission functions, i.e.,

$$\tau(u^*,\ \bar{T})=\tau_{H_2O}(u^*_{H_2O},\ \bar{T})\tau_{CO_2},\ \bar{T})\tau_{O_3}(u^*_{O_3},\ \bar{T}) \tag{13.11}$$

and

$$\tilde{\tau}(u^*,\ T_c)=\tilde{\tau}_{H_2O}(u^*_{H_2O},\ T_c)\tilde{\tau}_{CO_2},\ T_c)\tilde{\tau}_{O_3}(u^*_{O_3},\ T_c) \tag{13.12}$$

13.2.3 Cloudless atmosphere

The vertical discretization of the atmosphere and the vertical index are shown in Fig. 13.2. With use of the notation

$$\begin{aligned}
&\tilde{\tau}_\ell=\tilde{\tau}_\ell(u^*_\infty-u^*_\ell-u^*_\ell,\ T_c)\\
&\tau_\ell=\tau_\ell(u^*_\infty-u^*_\ell,\ \bar{T})\\
&\tau_{\ell',\ell}=\tau(|u^*_{\ell'}-u^*_\ell|,\ \bar{T})\equiv\tau_{\ell,\ell'}
\end{aligned} \tag{13.13}$$

Eqs. (13.9) and (13.10) may be expressed respectively as

$$R^{\downarrow}_{\ell} = \pi B_{\ell} - \pi B_c \tilde{\tau}_{\ell} - (\pi B_T - \pi B_c)\tau_{\ell} + \int_{\pi B_{\ell}}^{\pi B_T} \tau(u^* - u^*_{\ell}, \bar{T}) d(\pi B) \tag{13.14}$$

and

$$R^{\uparrow}_{\ell} = \pi B_{\ell} + \int_{\pi B_{\ell}}^{\pi B_{LM+1}} \tau(u^*_{\ell} - u^*, \bar{T}) d(\pi B) + (\pi B_g - \pi B_{LM+1})\tau_{\ell, LM+1} \tag{13.15}$$

Let $C_{\ell',\ell}$ represent the contribution to the flux at the upper level of layey ℓ from the layer ℓ', then $C_{\ell',\ell}$ can be evaluated by the trapezoidal low,

$$C_{\ell',\ell} = \int_{\pi B_{\ell}}^{\pi B_{\ell'+1}} \tau(|u^* - u^*_{\ell}|, \bar{T}) d(\pi B) = \frac{1}{2}(\tau_{\ell'+1,\ell} + \tau_{\ell',\ell})(\pi B_{\ell'+1} - \pi B_{\ell'}) \tag{13.16}$$

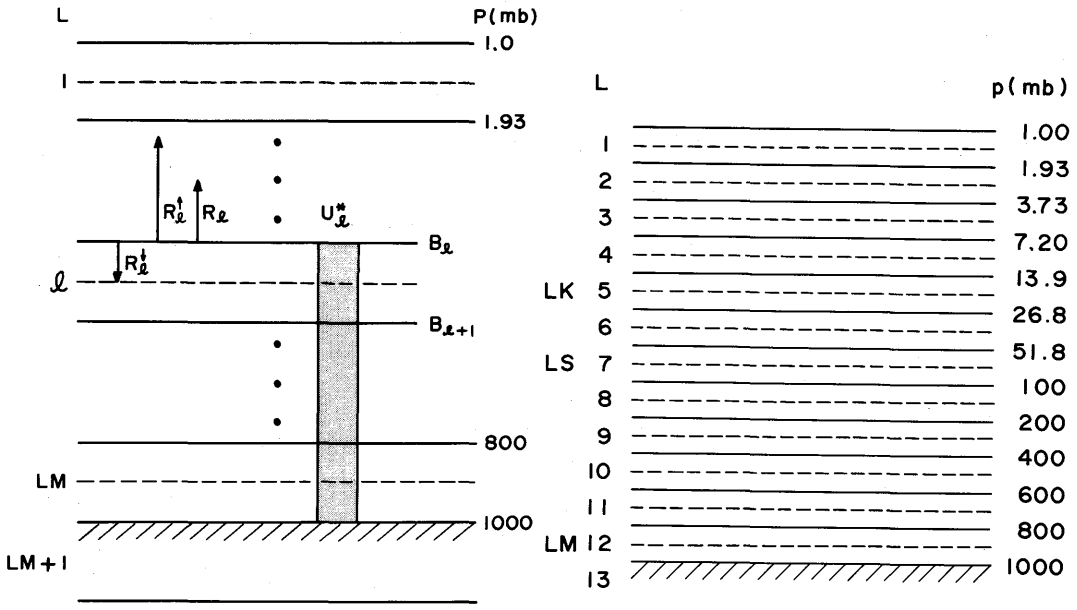

Fig. 13.2 (a) Indexing scheme for the long wave radiation calculation. The effective absorber amount u^*_{ℓ} is defined between the earth's surface and the top level of layer ℓ, (see eq. (13.7)). (b) Vertical discretization of the 12-layer MRI • GCM-I. The lowest five layers are same as that of the troposheric version of the MRI • GCM-I. LM is the index of the middle level of the lowest layer and LS is that of the lowest stratospheric layer. LK defines the level above which we use Dickinson (1973)'s longwave parameterization. Currently we adopt the value LM=12, LS=7 and LK=5 for the 12-layer model, and LM=5 and LS=0 for the 5-layer model.

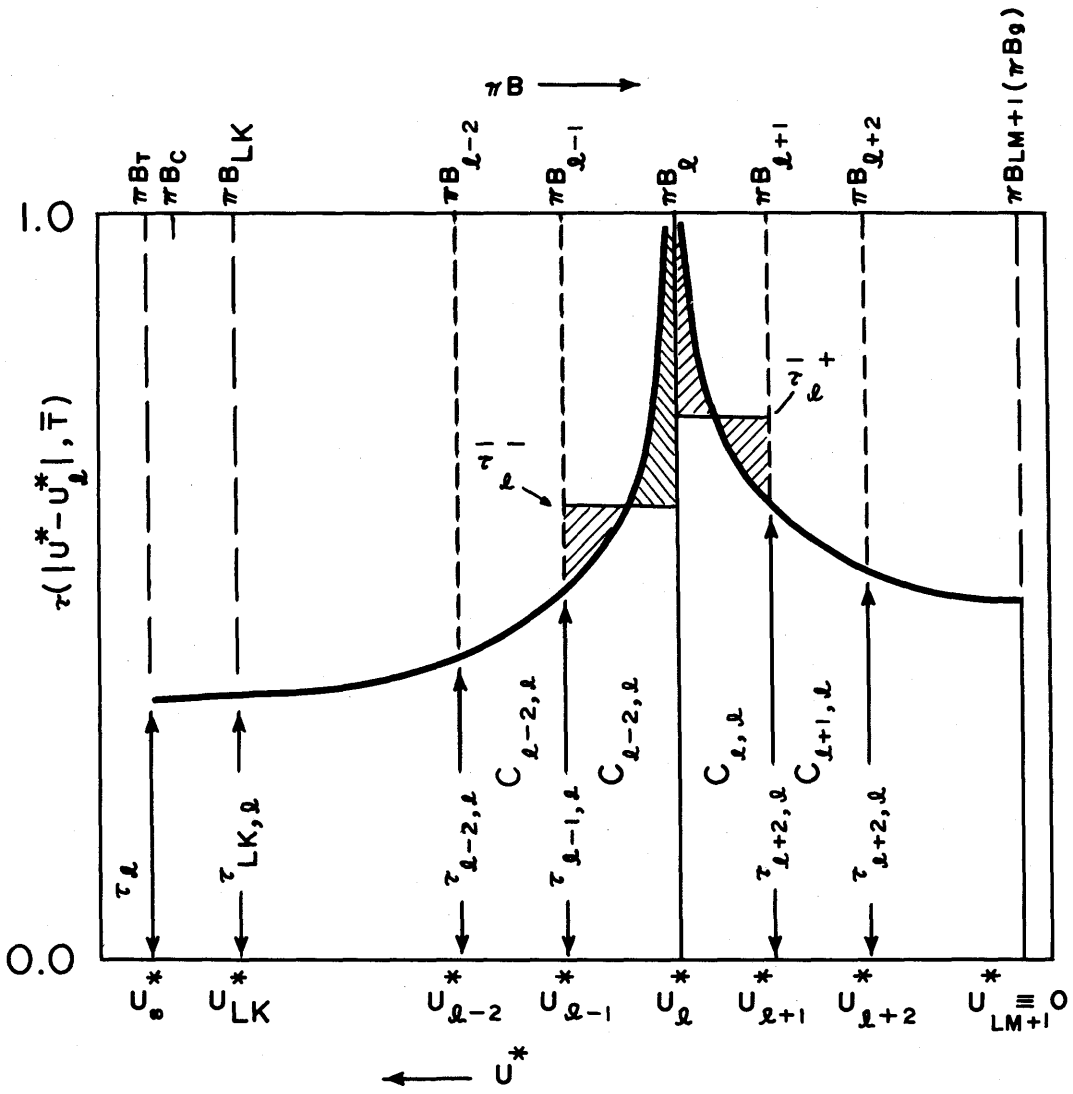

Fig. 13.3 Schematic representation of the transmission functions $\tau(\,|\,u^*-u^*_\ell\,|\,,\,\bar{T})$ and $\bar{\tau}^{\pm}_\ell$ at layer ℓ.

This form is approximately valid except when $\ell' = \ell + 1$ and $\ell' = \ell$. When the two layers are adjacent to each other, τ does not vary linearly with πB. Therefore, following Katayama (1972), two bulk transmission functions $\bar{\tau}^{\pm}_\ell$ are defined as follows,

$$\bar{\tau}^{-}_\ell \equiv (\pi B_\ell - \pi B_{\ell-1})^{-1} C_{\ell-1,\ell} \tag{13.17}$$

$$\bar{\tau}^{+}_\ell \equiv (\pi B_{\ell+1} - \pi B_\ell)^{-1} C_{\ell,\ell} \tag{13.18}$$

Fig. 13.3 shows a schematic representation of $\tau(\,|\,u^*-u^*_\ell\,|\,,\,\bar{T})$ and $\bar{\tau}^{\pm}_\ell$.

Substituting (13.16), (13.17) and (13.18) into (13.14) and (13.15), we obtain

$$R_\ell^{\downarrow} = \pi B_\ell - (\pi B_\ell - \pi B_{\ell-1})\bar{\tau}_\ell^{-} - \frac{1}{2}\sum_{\ell'=\ell-2}^{LK}(\tau_{\ell'+1,\ell} + \tau_{\ell',\ell} - \pi B_{\ell'})$$

$$-(\pi B_{LK} - \pi B_T)\tau_{LK,\ell} - (\pi B_T - \pi B_c)\tau_\ell - \pi B_c\tilde{\tau}_\ell \qquad (13.19)$$

and

$$R_\ell^{\uparrow} = \pi B_\ell + (\pi B_{\ell+1} - \pi B_\ell)\bar{\tau}_\ell^{+} + \frac{1}{2}\sum_{\ell'=\ell+1}^{LM}(\tau_{\ell'+1,\ell} + \tau_{\ell',\ell})(\pi B_{\ell'+1} - \pi B_{\ell'})$$

$$+(\pi B_g - \pi B_{LM+1})\tau_{\ell,LM+1} \qquad (13.20)$$

Currently LK=5 and LM=12 in the 12-L model. Above the level LK, we use Dickinson (1973) 's parameterization of long wave radiative cooling described in section 13.7. In the 5-L model, LK=1 and LM=5.

13.2.4 Cloudy atmosphere

Five types of clouds are identified currently. They are schematically shown in Fig. 13.4 and are classified as 1) clouds associated with large-scale condensation, 2) cirrus associated with sub-grid-scale deep cumulus convection, 3) sub-grid-scale penetrative cumulus convection, 4) clouds associated with middle level convection, and 5) stratus clouds associated with supersaturation within the planetary boundary layer. Currently only the first two types of clouds explicitly interact with radiation. Clouds are treated as black body radiators with a fractional cloudiness CL_ℓ equals to unity, except when the cloud layers are above 400 mb or colder than −40°C. In the latter case, clouds are considered to be in ice phase (*i.e.*, cirrus), and the fractional cloudiness CL_ℓ is assigned the value 0.5. Thus, for a cloudy atmosphere (13.19) and (13.20) are modified to

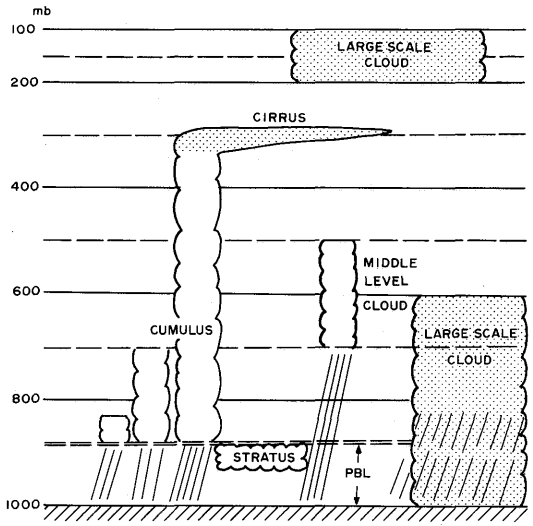

Fig. 13.4 Various types of clouds identified in the MRI • GCM-I. Radiatively interactive clouds are shaded.

$$R^{\downarrow}_{\ell} = \pi B_{\ell} - (\pi B_{\ell} - \pi B_{\ell-1})\bar{\pi}^{-}_{\ell}(1-CL_{\ell-1})$$

$$-\frac{1}{2}\sum_{\ell'=\ell-2}^{LK}(\tau_{\ell'+1,\ell})(\pi B_{\ell'+1} - \pi B_{\ell'})\prod_{k=\ell-1}^{\ell'}(1-CL_k)$$

$$-[(\pi B_{LK} - \pi B_T)\tau_{LK,\ell} + (\pi B_T - \pi B_c)\tau_{\ell} + \pi B_c \tilde{\tau}_{\ell}]\prod_{k=\ell-1}^{LK}(1-CL_k) \qquad (13.21)$$

$$R^{\uparrow}_{\ell} = \pi B_{\ell} + (\pi B_{\ell+1} - \pi B_{\ell})\bar{\tau}^{-}_{\ell}(1-CL_{\ell})$$

$$+\frac{1}{2}\sum_{\ell'=\ell+1}^{LM}(\tau_{\ell'+1,\ell} + \tau_{\ell',\ell})(\pi B_{\ell'+1} - \pi B_{\ell'})\prod_{k=\ell}^{\ell'}(1-CL_k)$$

$$+(\pi B_g - \pi B_{LM+1})\tau_{\ell,LM+1}\prod_{k=\ell}^{LM}(1-CL_k) \qquad (13.22)$$

13.2.5 Effective absorber amounts

13.2.5.a Water vapor

The effective absorber amount u* is given by (13.7). The water vapor mixing ratio q_{H_2O} (p) is a prognostic variable which is calculated by the way described in Chapters 6, 7 and 9. Pressure scaling lows were originally incorpolated to replace an inhomogeneous optical path with an equivalent homogeneous optical path. Since this is an empirical method, there is some uncertainty in the value of the pressure scaling factor α_{H_2O}. In Table 13.1 the values of α_{H_2O} which is adopted by various authors are tabulated. Currently α_{H_2O} is assumed to be 0.9 atter McClatchey *et al.* (1972), who found a best fit to laboratory and theoretical data for that value.

Table 13.1 Pressure scaling factor for water vapor adopted by various authors.

	MANABE *et al.* (1967)	SASAMORI (1968)	KATAYAMA (1972)	McCLATCHEY *et al.* (1972)
α_{H_2O}	0.7	1.0	0.6	0.9

13.2.5.b Carbon dioxide

For carbon dioxide, (13.7) is slightly modified as

$$u^*_{CO_2}(p) = \frac{1}{g\rho_{CO_2,NTP}}\int_{P}^{Ps} q_{CO_2}(p')\left(\frac{p'}{p_o}\right)^{\alpha_{CO_2}} dp' \qquad (13.23)$$

where $\rho_{CO_2,NTP} = 1.977$ kg m^{-3} is the carbon dioxide density at NTP. The mixing ratio of CO_2

is assumed to be constant both in space and time, and is assigned the value 0.0489 percent by weight ($q_{CO_2}=4.89\times10^{-4}$), or 0.032 percent by volume (320PPM). Thus

$$u^*_{CO_2}(p)=\frac{252}{\alpha_{CO_2}+1}\left[\left(\frac{p_s}{p_o}\right)^{\alpha_{CO_2}+1}-\left(\frac{p}{p_o}\right)^{\alpha_{CO_2}+1}\right] \tag{13.24}$$

Following Manabe and Möller (1961), α_{CO_2} is taken as 0.86.

13.2.5.c Ozone

The ozone mixing ratio $q_{O_3}(p)$ is predicted in a way described in Chapters 6 and 12. The predicted amount is used for the radiation calculation. The effective absorber amount of ozone is also given by (13.23) by replcing $\rho_{CO_2,NTP}$ and α_{CO_2} with $\rho_{O_3,NTP}=2.144$ kg m^{-3} and $\alpha_{O_3}=0.3$ respectively, after Manabe and Möller (1961).

Thus,

$$u^*_{O_3,\ell}=\frac{1}{g\rho_{O3NTP}}\sum_{\ell'=\ell}^{LM} q_{O_3,\ell}\int_{P_{\ell'}}^{P_{\ell'+1}}\left(\frac{p'}{p_o}\right)^{\alpha_{O3}}dp' \tag{13.25}$$

13.2.6 Empirical transmission function equations

13.2.6.a Water vapor

Total transmission function of a mixture of gases is given by (13.11) and (13.12). Yamamoto (1952) calculated τ and $\tilde{\tau}$ for water vapor from experimental laboratory data. Katayama (1972) obtained the empirical transmission functions for $\tau_{H_2O}(u^*_{H_2O}, \bar{T})$ by taking an average of τ given by Yamamoto (1952) for T=220°K, 260°K, and 300°K, *i.e.*,

$$\tau_{H_2O}(u^*, T)=\begin{cases}0.373-0.274Z+0.035Z^2, & (u^*\geq 1)\\ 0.373-0.2595Z-0.0275Z^2, & (10^{-4}\leq u^*<1)\\ F(298.7, 1.0), & (u^*<10^{-4})\end{cases} \tag{13.26}$$

where $F(a,b)=1/(1+au^{*b})$ and $Z=\log_{10}u^*$.

And for $\tilde{\tau}_{H_2O}(u^*, T_c)$

$$\tilde{\tau}_{H_2O}(u^*, 220°K)=\begin{cases}0.254-0.1985Z+0.0205Z^2, & (u^*\geq 0.1)\\ 0.216-0.2827Z-0.0258Z^2, & (10^{-4}\leq u^*<0.1)\\ F(2.56, 0.39), & (u^*<10^{-4})\end{cases} \tag{13.27}$$

13.2.6.b Carbon dioxide and ozone

We adopt empirical transmission function equations derived by Schlesinger (1976) both for 15μ band of carbon dioxide and for 9.6μ band of ozone based on the experimental

laboratory measurements by Elsasser (1960).

$$\tau_{CO_2}(u^*_{CO_2}, T) = 0.924 - 0.0390Z - 0.00466Z^2 \tag{13.28}$$

$$\tau_{O_3}(u^*_{O_3}, T) = 0.919 - 0.0252Z - 0.000998Z^2 \tag{13.29}$$

where Z equals to $\log_{10}u^*_{CO_2}$ for (13.28) and $\log_{10}u^*_{O_3}$ for (13.29). $\tau_{CO_2}(u^*_{CO_2}, \bar{T})$ and $\tau_{O_3}(u^*_{O_3}, \bar{T})$ are defined as the arithmetic mean of τ_{CO_2} and τ_{O_3} over $-80°C$ to $40°C$.

13.2.6.c Bulk transmission functions

Katayama (1972) introduced the bulk transmission functions $\bar{\tau}^{\pm}_{\ell}$ by (13.17) and (13.18) which are evaluated by linear interpolation between $\bar{\tau}^{\pm}_{\ell}=1$ for $|u^*-u^*_{\ell}|=0$ and $\bar{\tau}^{\pm}_{\ell}=\bar{\tau}_{\ell\pm1,\ell}$ as,

$$\bar{\tau}^{\pm}_{\ell} = (1+m^{\pm}_{\ell}\,\tau_{\ell\pm1,\ell})/(1+m^{\pm}_{\ell}) \tag{13.30}$$

The linear interpolation factors $m^{\pm}_{\ell}$ must be determined by the physical parameters of the adjacent layers. Katayama (1972) determined $m^{\pm}_{\ell}$ once and for all by numerical experiments in which trapezoidal integration scheme (13.17) was evaluated numerically by subdividing the layer under consideration into thin sublayers of 10 mb thickness. In this calculation, the vertical distribution of the water vapor mixing ratio q and the temperature T in an adjacent layer are assumed to be

$$q = q_{\ell}(p/p_{\ell})^{k_{\ell}} \tag{13.31}$$

$$T = T_{\ell} + \gamma_{\ell}(p-p_{\ell})$$

We follow Katayama's (1972) numerical experiment. He could express $m^{\pm}_{\ell}$ approximately as a linear function of Δp, the depth of layer in mb, when the remaining parameters are fixed. Thus,

$$m^{\pm}_{\ell} = a^{\pm}_{\ell} + b^{\pm}_{\ell}\,\Delta p/100. \tag{13.32}$$

$a^{\pm}_{\ell}$ and $b^{\pm}_{\ell}$ are obtained empirically,

$$a^{+}_{\ell} = L^{+}_{a}(p_{\ell}) + F^{+}_{a}(z_{\ell})$$

$$b^{+}_{\ell} = L^{+}_{b}(p_{\ell}) + F^{+}_{b}(z_{\ell}) + \left(\frac{\partial b}{\partial k}\right)^{+}\Delta k_{\ell} + \left(\frac{\partial b}{\partial k}\right)^{+}\Delta\gamma_{\ell} \tag{13.33}$$

where $\Delta k = k_{\ell} - 3$, $\Delta\gamma_{\ell} = \gamma_{\ell} - 10$ (°K/100 mb), and

$$L^{+}_{a}(p_{\ell}) = -1.66 + 1.76\,\log_{10}p_{\ell}, \tag{13.34}$$

$$L^{+}_{b}(p_{\ell}) = -0.197 + 0.0002\,p_{\ell},$$

$$F^{+}_{a}(Z_{\ell}) = 0.30\,Z_{\ell} + 0.28\,Z^2_{\ell} + 0.04\,Z^3_{\ell}, \tag{13.35}$$

$$F^{+}_{b}(Z_{\ell}) = 0.0812\,Z_1 - 0.045\,Z_1^2 + 0.02334\,Z_1^3,$$

$$\left(\frac{\partial b}{\partial k}\right)^{+}=\mathrm{Min}(-0.041+0.021\ Z_{\ell}, -0.006)<0,$$

$$\left(\frac{\partial b}{\partial \gamma}\right)^{+}=\mathrm{Max}(0.01225+0.007\ Z_{\ell}, 0.0093)>0, \tag{13.36}$$

$$a^{-}_{\ell}=-0.09L^{-}_{a}(p_{\ell})+F^{+}_{a}(Z_{\ell}-0.105L^{-}_{a}(p_{\ell})), \tag{13.37}$$

$$b^{-}_{\ell}=-0.09L^{-}_{b}(p_{\ell})+F^{-}_{b}(Z_{\ell}-0.105L^{-}_{b}(p_{\ell}))+\left(\frac{\partial b}{\partial k}\right)^{-}\Delta k_{\ell}+\left(\frac{\partial b}{\partial \gamma}\right)^{-}\Delta\gamma_{\ell}$$

$$L^{-}_{a}(p_{\ell})=\mathrm{Max}(61.86-22.92\ \log_{10}p_{\ell}, 76.63-28.39\ \log_{10}p_{\ell}), \tag{13.38}$$

$$L^{-}_{b}(p_{\ell})=\mathrm{Min}(-42.59+15.78\ \log_{10}\ p_{\ell}, -60.81+22.53\ \log_{10}\ p_{\ell}),$$

$$F^{-}_{a}(X)=2.57+0.233\ X+0.18\ X^{2}+0.027\ X^{3}, \tag{13.39}$$

$$F^{-}_{b}(X)=1.42+0.48\ X+0.16\ X^{2}+0.011\ X^{3},$$

$$\left(\frac{\partial b}{\partial k}\right)^{-}=0.08+(0.371-0.102\ \log_{10}\ p_{\ell})(z_{\ell}+2.1)>0,$$

$$\left(\frac{\partial b}{\partial r}\right)^{-}=\mathrm{Min}(-0.0325-0.005z_{\ell}, -0.0275)<0, \tag{13.40}$$

In the above $Z_{\ell}=\log_{10}\ q_{\ell}$, $Z_{1}=\mid Z_{\ell}+2.5\mid$, and X is a dummy variable.

Recall that $\bar{\tau}^{\pm}_{\ell}$ were introduced due to the failure of the trapezoidal integration scheme for the layers adjacent to the level under consideration. τ varies more rapidly with πB than a linear relationship within these layers. This nonlinear character of τ is most pronounced in the troposhere where water vapor is abundant. However in the stratosphere where water vapor is less impotant, πB is more uniform (Schlesinger, 1976). Thus,

$$m^{\pm}_{\ell}=1 \qquad \ell \leq \mathrm{LS} \tag{13.41}$$

is assumed above 100 mb level.

13.2.7 Long wave radiative cooling in the upper stratoshere

Although Katayama's method of using mean transmission functions (13.5) and (13.6) is good in the troposhere and also in the lower stratoshere, it is less so in the upper stratosphere where unisotropy of radiative flux dominates. As a substitute of Katayama's method, we adopt Dickinson (1973)'s long wave radiative cooling parameterization in the upper stratoshere (*i. e.* the region above 13.9 mb in the current 12 layer version. See Fig. 13.2). That is

$$\left(\frac{\partial T_{\ell}}{\partial t}\right)_{tr}=-C_{o,\ell}-a_{o,\ell}(T_{\ell}-T_{o,\ell})\beta_{\ell} \tag{13.42}$$

where

$$\beta_\ell = \begin{cases} 1, & \text{if } | T_\ell - T_{o,\ell} | \leq 5°K \\ 1+\dfrac{0.0033(T_\ell - T_{o,\ell})}{T_{o,\ell}-135} & \text{if } | T-T_{o,\ell} | > 5°K \text{ and } T_\ell \geq 130°K \\ \dfrac{e^{-960/T_\ell}-e^{-960/To,\ell}}{960e^{-960/To,\ell}(T_\ell - T_{o,\ell})}T^2_{o,\ell} & \text{if } | T_\ell - T_{o,\ell} | > 5°K \text{ and } T_\ell < 130°K \end{cases} \quad (13.43)$$

$C_{o,\ell}$ is the cooling rate expected for the reference temperature profile $T_{o,\ell}$, and $a_{o,\ell}$ is a Newtonian cooling coefficient. As for a reference temperature $T_{o,\ell}$, the 1962 standard atmosphere profile is adopted. β_ℓ is a modification factor introduced by Dickinson and revised by Schlesinger (1976).

The values of $T_{o,\ell}$, $C_{o,\ell}$ and $a_{o,\ell}$ for the upper four layers are presented in Table 13.2.

Table 13.2 Values used in the Dickinson's long wave cooling parameterization.

k	p (mb)	$T_{o,\ell}$ (K)	$C_{o,\ell}$ (K DAY^{-1})	$a_{o,\ell}$ (DAY^{-1})
1	1.39	265.73	9.47	0.180
2	2.68	251.81	6.14	0.127
3	5.18	238.57	4.17	0.0993
4	10.0	227.72	2.62	0.0755

13.3 Solar radiation

13.3.1 Basic quantities

The extraterrestrial solar flux incident on a horizontal surface is given by

$$S=\bar{S}_o\left(\frac{\bar{\gamma}_E}{\gamma_E}\right)^2\cos\zeta \quad (13.44)$$

where

$$\cos\zeta=\sin\phi\sin\delta+\cos\phi\cos\delta\cos h, \quad (13.45)$$

$S_o=1345$ watt m^{-2} is the solar constant at one astronomical unit $\bar{\gamma}_E$, γ_E is the earth−sun distance, ζ is the solar zenith angle, ϕ is the latitude, δ is the solar declination and h is the hour angle of the sun. As shown in Appendix A13.1, δ and γ_E can be determined by a perturbation of Kepler's second low. The hour angle at each grid point is updated at every

diabatic time step, and the solar declination and earth−sun distance are updated once a simulated day.

In the solar radiation parameterization developed by Katayama (1972) and Schlesinger (1976), the solar flux under cloudless conditions is depleted only by water vapor and ozone absorption and Rayleigh scattering. The effective absorption bands of water vapor for the solar spectrum exist in the wave length range $\lambda > 0.9\mu$. As the amount of Rayleigh scattering varies as λ^{-4}, the scattering in that range can be neglected. As for ozone, the absorption bands exist in the wavelength range $\lambda < 0.8\mu$. Because the amount of Rayleigh scattering increases exponentially with pressure, and because the heating by ozone absorption below 200 mb is negligible compared to the heating by water vapor absorption, we can neglect the effect of Rayleigh scattering on ozone absorption above 200 mb and also neglect the effect of ozone absorption on Rayleigh scattering below 200 mb.

Following Joseph (1966, 70) and based upon above considerations, the solar radiation is divided into two parts. One is "the scattered part",

$$S_0^s = 0.634\ S_o \cos\zeta \qquad 0.9\mu > \lambda \tag{13.46}$$

and the other "the absorbed part",

$$S_0^a = 0.366\ S_o \cos\zeta \qquad \lambda > 0.9\mu \tag{13.47}$$

13.3.2 Absorptivity of water vapor

Schlesinger (1976) calculated water vapor absorptivity A_{H_2O} from the data of McClatchey *et al.* (1972) and approximated the absorptivity piecewisely by quadratic polynomials;

$$A'_{H_2O}(X) = a_i + b_i X + C_i X^2 \qquad X_{i-1} \leq X < X_i \tag{13.48}$$

$$A_{H_2O}(X) = A'_{H_2O}(X)/0.366 \tag{13.49}$$

$$X = u^* M \tag{13.50}$$

where the effective water vapor amount u^* is given by (13.7),

$$M = 35 \sec\zeta \,/\, \sqrt{1224 + \sec^2\zeta} \tag{13.51}$$

is the magnification factor after Rodgers (1967), with sphericity. $A_{H_2O}(X)$ is the absorptivity for the "absorbed" part, and $A'_{H_2O}(X)$ is the absorptivity for the total solar spectrum. The coefficients a_i, b_i, and c_i are presented in Appedix A13.2.

By letting $y = A'_{H_2O}(X)$, the inverse function $X = A'^{-1}_{H_2O}(y)$ was fitted into quadratic polynomials;

$$X = A^{-1}_{H_2O}(y) = d_j + e_j y + f_j y^2, \qquad y_{j-1} < y \leq y_j \tag{13.52}$$

The coefficients d_j, e_j, and f_j are also presented in Appendix A13.2.

13.3.3 Absorptivity of ozone

The absorptivity function of ozone for the total solar spectrum was calculated by Schlesinger (1976) and was fitted by quadratic polynomials;

$$A'_{O_3}(X) = a_i + b_i X + C_i X^2 \qquad X_{i-1} < X \leq X_i \tag{13.53}$$

$$A_{O_3}(X) = A'_{O_3}(X)/0.634 \tag{13.54}$$

where $A_{O_3}(X)$ is absorptivity for the "scattered" part, $A'_{O_3}(X)$ is the absorptivity for the entire solar spectrum and

$$X = u^*_{O_3} M$$

The coefficients a_j, b_j, and c_j are tabulated in Appendix A13.3.

The effective ozone amount $u^*_{O_3}$ is calculated by, (cf. eq. (13.21))

$$u^*_{O_3} = \frac{1}{\rho_{O3,NTP}} \int_o^z \rho_{O_3}(z)dz = \frac{1}{g\rho_{O3,NTP}} \int_o^p p_{O_3}(p')dp' \tag{13.55}$$

where ρ_{O_3} is the ozone density, q_{O_3} is the ozone mixing ratio and $\rho_{O_3,NTP} = 2.144$ kg m^{-3} is the ozone density at NTP. In a discrete case, (13.55) can be written as,

$$u^*_{O_3,\ell} + \frac{1}{g\rho_{O3,NTP}} \sum_{\ell'=1}^{\ell} q_{O_3,\ell'}(p_{\ell'+1} - p_{\ell'}) \tag{13.56}$$

where $p_{\ell'}$ is the pressure at the upper surface of layer ℓ', $q_{O_3,\ell'}$ the predicted ozone mixing ratio for layer ℓ', and

$$u^*_{O_3,\ell} = \frac{1}{\rho_{O3,NTP}} \int_{z0.5}^{\infty} \rho_{O_3}(z)dz \tag{13.57}$$

In calculating (13.57), we assume that ozone number density $n_{O_3}(z)$ above the top level of the model $z_{0.5}$ decays exponentially with altitude following the mean ozone distribution by Krueger (1973). Thus,

$$n^*_{O_3}(z) = n_{O_3}(z_1) \exp\left(\frac{z - z_1}{H}\right) \qquad z \geq z_1 \tag{13.58}$$

where Z_1 is the altitude of the midlevel of layer 1, and $H = 4.35$ km. Substituting (13.58) into (13.57) gives

$$u^*_{O_3,\ell} = \frac{H \exp\left(-\frac{z_{0.5} - z_1}{H}\right) q_{O_3,\ell} p_{1.5}}{\rho_{O_3,NTP} R T_1} \tag{13.59}$$

Where $p_{1.5}$ and T_1 are pressure and temperature at the midlevel of layer 1 respectively, and

R is gas constant.

13.3.4 Cloudless atmosphere

13.3.4.a "Absorbed" part

The "absorbed" part of the solar radiation S_0^a is absorbed only by the water vapor in the troposhere and at the earth's surface. The other absorption can be neglected. (*e.g.* The absorption by the water vapor in the stratoshere can be neglected in comparison to the "scattered" part absorption by ozone.)

After neglecting the absorption by water vapor on the radiation reflected by the earth's surface, the net downward flux of the "absorbed" part at the upper surface of layer ℓ, $S_{a,\ell}$, is

$$S_{a,\ell} = S_0^a \qquad \ell = 1,\cdots\cdots,LS \tag{13.60}$$

$$S_{a,\ell} = S_0^a\{1 - A_{H_2O}[(u^*_{H_2O,\infty} - u^*_{H_2O,\ell})M]\} \qquad \ell = LS+1,\cdots\cdots,LM+1$$

where A_{H_2O} was given by (13.48) and (13.49). The absorption of solar radiation by water vapor in layer ℓ, $AS_{a,\ell}$, is therefore

$$\begin{aligned} AS_{a,\ell} &= 0.0, && \ell = 1,\cdots\cdots, LS \\ AS_{a,\ell} &= S_{a,\ell} - S_{a,\ell+1}, && \ell = LS+1,\cdots\cdots, LM \end{aligned} \tag{13.61}$$

The absorption of the solar radiation that is absorbed at the earth's surface is

$$AS_{a,LM+1} = (1-\alpha_s)S_{a,LM+1} \tag{13.62}$$

where α_s is the albedo of the surface, which is given in Table 13.3.

13.3.4.b "Scattered" part

By neglecting the effect of Rayleigh scattering on ozone absorption above 200 mb, the downward flux and the absorption of the downward flux of the scattered part are

$$S^{\downarrow}_{s,\ell} = S_0^s\{1 - A_{O_3}(u^*_{O_3,\ell}M)\} \tag{13.63}$$

$$AS^{\downarrow}_{s,\ell} = S^{\downarrow}_{s,\ell} - S^{\downarrow}_{s,\ell+1} \quad , \quad \ell = 1,\cdots\cdots, LS+1$$

$$AS^{\downarrow}_{s,\ell} = 0.0 \quad , \quad \ell = LS+2,\cdots\cdots, LM \tag{13.64}$$

where the effective ozone amount $u^*_{O_3,\ell}$, is given by (13.56) and (13.59).

By neglecting the effect of ozone absorption on Rayleigh scattering below 200 mb, the downward flux of the "scattered" part at the earth's surface, $S^{\downarrow}_{s,LM+1}$ is

$$S_{s,LM+1} = S^{\downarrow}_{s,LS+2}(1-\alpha_o)/(1-\alpha_o\alpha_s) \tag{13.65}$$

where

Table 13.3 Surface albedo adopted in the MRI•GCM-I.

Surface condition	Albedo
open ocean	0.07
bare land	0.14
frozen land	0.3
permanent land ice and snow	Min (0.85, 0.7+0.15 h) where h is height in km
bare sea ice	0.4
snow on sea ice	0.7
melting snow	0.5

$$\alpha_o = 0.085 - 0.247 \log_{10}\left(\frac{P_s}{1000}\cos\xi\right) \tag{13.66}$$

is the albedo due to Rayleigh scattering. (Coulson, 1959)

The "scattered" part of the solar radiation that is absorbed at the earth's surface is

$$AS^{\downarrow}_{s,LM+1} = (1-\alpha_s)S^{\downarrow}_{s,LM+1} \tag{13.67}$$

The upward flux of the "scattered" part at LS+2, $S^{\downarrow}_{s,LS+2}$, is

$$\begin{aligned} S^{\downarrow}_{s,LS+2} &= S^{\downarrow}_{s,LS+2} - AS^{\downarrow}_{s,LM+1} \\ &= S^{\downarrow}_{s,LS+2}\{1-(1-\alpha_s)(1-\alpha_o)/(1-\alpha_o\alpha_s)\} \end{aligned} \tag{13.68}$$

By neglecting the effect of Rayleigh scattering on ozone absorption above 200 mb, the absorption of upward flux of the "scattered" part in layer ℓ, $AS_{a,\ell}$ is

$$\begin{aligned} AS^{\uparrow}_{s,\ell} = S^{\uparrow}_{s,LS+2}\{&A_{O_3}[u^*_{O_3,LS+2}M + 1.9(u^*_{O_3,LS+2} - u^*_{O_3,\ell})] \\ &- A_{O_3}[u^*_{O_3,LS+2}M + 1.9(u^*_{O_3,LS+2} - u^*_{O_3,\ell+1})]\}, \quad \ell = 1,\cdots\cdots, LS+1 \end{aligned} \tag{13.69}$$

$$AS^{\uparrow}_{s,\ell} = 0.0 \quad , \quad \ell = LS+2,\cdots\cdots, LM$$

where the factor 1.9 is an average magnification factor for the diffuse upward radiation. (Lacis and Hansen, 1974)

The heating rate due to absorption of solar radiation at layer ℓ is given by

$$\left(\frac{\partial T}{\partial t}\right)_{sr,\ell} = \frac{g(AS_{a,\ell} + AS^{\downarrow}_{s,\ell} + AS^{\uparrow}_{s,\ell})}{c_p(p_{\ell+1} - p_\ell)} \tag{13.70}$$

where p_ℓ is the pressure at the upper surface of layer ℓ. (*cf.* (13.4))

13.3.5 Cloudy atmosphere

13.3.5.a Single cloud

Consider a single cloud located in layer L as shown in Fig. 13.5. The flux of the "absorbed" part at the upper surface of layer $\ell \leq L$, $S_{a,\ell}$, is given by (13.60) as

$$S_{a,\ell} = S_o^a\{1 - A_{H_2O}[(u^*_{H_2O,\infty} - u^*_{H_2O,\ell})M]\} \tag{13.71}$$

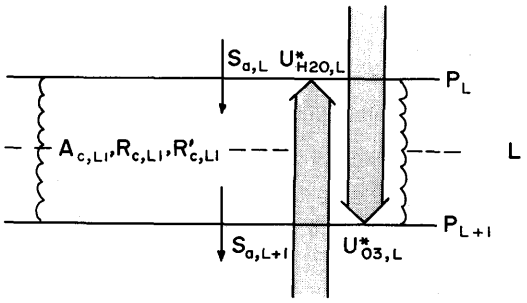

Fig. 13.5 A single cloud layer. $u^*_{H_2O,\ell}$ follows the definition of eq. (13.7), while $u^*_{H_2O,\ell}$ defined as the effective ozone absorber amount between the bottom level of layer ℓ and top of the atmosphere.

By letting $A_{c,L}$ and $R_{c,L}$ denote the absorptivity per unit pressure thickness and the reflectivity of cloud layer L, the flux of the "absorbed" part at the upper surface of layer L+1, $S_{a,L+1}$, is given by

$$S_{a,L+1} = [1 - R_{c,L} - A_{c,L}(p_{L+1} - P_L)]S_{a,L} \tag{13.72}$$

where the quantity in brackets represents the transmissivity of cloud layer L. In order to calculate the fluxes beneath the cloud by (13.71), the total optical thickness from the top of the atmosphere to the upper surface of the layer under consideration is required. Katayama (1972) defined the equivalent total optical thickness of water vapor from the top of the atmosphere to the base of the cloud layer L, Γ_{L+1}, by

$$(1 - R_{c,L})S_o^a\{1 - A_{H_2O}(\Gamma_{L+1})\} = S_{a,L+1}, \tag{13.73}$$

hence

$$\Gamma_{L+1} = A^{-1}_{H_2O}\left(1 - \frac{S_{a,L+1}}{(1 - R_{c,L})S_o^a}\right) \tag{13.74}$$

where $A^{-1}_{H_2O}$ is the inverse of the water wapor absorbtivity function given by (13.52). The flux across the upper surface of any layer beneath the cloud base is, then, given by

$$S_{a,\ell} = (1 - R_{C,L})S_o^a\{1 - A_{H_2O}[\Gamma_{L+1} + 1.66(u^*_{H_2O,L+1} - u^*_{H_2O,\ell})]\} \tag{13.75}$$

where 1.66 is the diffusivity factor for diffuse radiation beneath the cloud. The absorption of solar radiation is

$$AS_{a,\ell} = \begin{cases} S_{a,\ell} - S_{a,\ell+1}, & \ell = LS+1, \cdots\cdots, LM \text{ except } \ell = L \\ (1 - R_{C,L})S_{a,L} - S_{a,L+1}, & \ell = L \end{cases} \tag{13.76}$$

where $R_{c,L}$ is the reflectivity of cloud layer L for the "absorbed" part, and $S_{a,L}$, the solar radiations reflected from the cloud layer. The absorption of radiation reflected from the

cloud layer is neglected. The "absorbed" part of the solar radiation that is absorbed at the earth's surface is given by (13.62).

In the case of "scattered" part of the solar radiation, equations (13.63), (13.64), (13.67), and (13.69) are unchanged. In equations (13.65) and (13.68), α_o is replaced by α_c, the albedo of the cloudy atmosphere for the "scattered" part,

$$\alpha_c = 1-(1-R'_{c,L})(1-\alpha_o) \tag{13.77}$$

where $R'_{c,L}$ is the reflectivity of cloud layer L for the "scattered" part.

13.3.5.b Two or more contiguous cloud layers, and multiple clouds

In the model, each cloud layer within two or more contiguous cloud layers is treated as a separate cloud for the solar radiation calculation like one of multiple clouds.

(A) "Absorbed" part

For simplicity, consider two clouds each consisting of a single layer. The cloud 1 lies in the layer L1 and the cloud 2 in the layer L2 (see Fig. 13.6). For layers $\ell \leq$ L1, $S_{a,\ell}$ is given by (13.60),

$$S_{a,\ell} = S^a_o\{1-A_{H_2O}[(u^*_{H_2O,\infty} - u^*_{H_2O,\ell})M]\}$$

$$\ell = LS+1, \cdots\cdots, LM+1 \tag{13.78}$$

By (13.72), $S_{a,L1+1}$ is

$$S_{a,L1+1} = [1-\bar{R}_{c,L1}-A_{c,L1}(p_{L1+1}-p_{L1})]S_{a,L1} \tag{13.79}$$

By (13.74), the equivalent total optical thickness from the top of the atmosphere to the base of cloud 1, Γ_{L1}, is

$$\Gamma_{L1} = A^{-1}_{H_2O}\left(1-\frac{S_{a,L1+1}}{(1-\bar{R}_{c,1})S^a_o}\right) \tag{13.80}$$

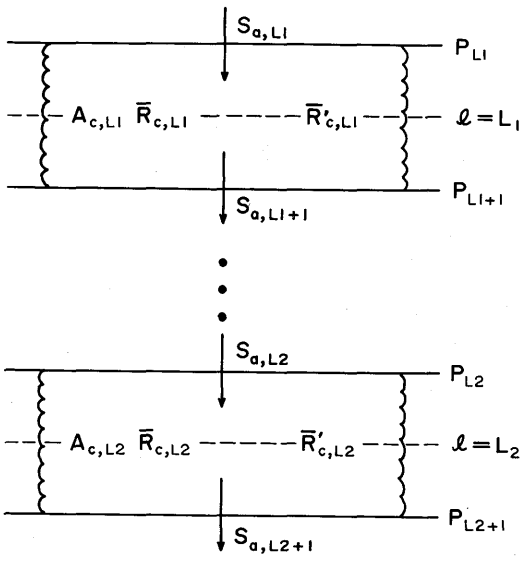

Fig. 13.6 Two separated cloud layers.

The flux across the upper surface of layers L1+2$\leq \ell <$L2 is given by (13.75)

$$S_{a,\ell} = (1-\bar{R}_{c,1})S^a_o\, A_{H_2O}[1-\{\Gamma_{L1}+1.66(u^*_{H_2O,L1+1}-u^*_{H_2O,\ell})\}] \tag{13.81}$$

$S_{a,L2+1}$ is given by

$$S_{a,L2+1} = [1-\bar{R}_{c,L2}-A_{c,L2}(p_{L2+1}-p_{L2})]S_{a,L2} \tag{13.82}$$

where use has been made of (13.72). The equivalent total optical thickness from the top of the atmosphere to the base of cloud 2, Γ_{L2}, is

$$\Gamma_{L2}=A_{H_2O}^{-1}\left\{1-\left(\frac{S_{a,L2+1}}{(1-\bar{R}_{c,1})(1-\bar{R}_{c,2})S_o^a}\right)\right\} \tag{13.83}$$

The solar flux incident on the lower cloud 2, $S_{a,L2}$, is affected by the existence of cloud 1 (see (13.79)). Then, from (13.82) and (13.83) Γ_{L2} differs from what it would be if cloud 1 did not exist ; that is, the equivalent total optical thickness is a function of the overlying cloud cover. The flux across the upper surface of layers $\ell \geq L2+2$ is

$$S_{a,\ell}=(1-\bar{R}_{c,2})(1-\bar{R}_{c,1})S_o^a\{1-A_{H_2O}[\Gamma_{L2}+1.66(u^*_{L2+1}-u^*_{\ell})]\}$$
$$\ell=L2+2,\cdots\cdots,LM+1 \tag{13.84}$$

The absorption of solar radiation, AS_ℓ, is

$$AS_{a,\ell}=\begin{cases} S_{a,\ell}-S_{a,\ell+1} & \ell=LS+1,\ldots,LM \\ & \text{but } \ell \neq L1 \text{ or } L2 \\ (1-\bar{R}_{c,j})S_{a,Lj}-S_{a,Lj+1}, & \ell=L1 \text{ and } L2 \end{cases} \tag{13.85}$$

The direct solar radiation in the "absorbed" part that reaches the earth's surface, $S^d_{a,LM+1}$ is

$$S^d_{a,LM+1}=(1-\bar{R}_{c,2})(1-\bar{R}_{c,1})S_o^a\{1-A_{H_2O}[\Gamma_{L2}+1.66u^*_{H_2O,L2+1}]\} \tag{13.86}$$

The indirect solar radiation in the "absorbed" part that reaches the earth's surface due to multiple reflections between the two clouds, $S^i_{a,LM+1}$, is

$$S^i_{a,LM+1}=(\bar{R}_{c,2}S_{a,L2})\left(\frac{\bar{R}_{c,1}}{1-\bar{R}_{c,1}\bar{R}_{c,2}}\right)(1-\bar{R}_{c,2})\left(\frac{1}{1-\alpha_s\bar{R}_{c,1,2}}\right) \tag{13.87}$$

$$\bar{R}_{c,1,2}=1-\left(\frac{(1-\bar{R}_{c,1})(1-\bar{R}_{c,2})}{1-\bar{R}_{c,1}\bar{R}_{c,2}}\right) \tag{13.88}$$

is the albedo of the two clouds (neglecting atmospheric absorption of the reflected radiation). The total solar radiation in the "absorbed" part reaching the earth's surface $S_{a,LM+1}$, is

$$S_{a,LM+1}=S^d_{a,LM+1}+S^i_{a,LM+1} \tag{13.89}$$

and the absorption by the earth's surface is given by (13.62).

The above equations may be generalized in a straightforward manner to the case of an arbitary number of cloud layers.

(B) "Scatterd" part

The treatment is the same as that described in subsection 13.3.5 but $\bar{R}'_{C,L}$ in (13.77) is replaced by $\bar{R}'_{C,1,2}$ which is given by (13.88) with $\bar{R}_{c,j}$ replaced by $\bar{R}'_{c,j}$.

13.3.6 The reflectivity and absorptivity of clouds

The reflectivities of the "absorbed" part R_c, and that of the "scattered" part R'_c, and the absorptivity per unit pressure thickness of the "absorbed" part A_c, and that of the "scattered" part A'_c, for cloud layer are assumed to be characterized by the respective properties of low, middle, or high clouds following Rodgers (1967) and Katayama (1972). That is

$$R_{c,\ell}(R'_{c,\ell}) = \begin{cases} 0.19(0.21), & \text{for } 100 \text{ mb} \leq p_\ell < 400 \text{ mb cirrus} \\ 0.46(0.54), & \text{for } 400 \text{ mb} \leq p_\ell < 800 \text{ mb and not cirrus} \\ 0.50(0.66), & \text{for } 800 \text{ mb} \leq p_\ell \text{ and not cirrus} \end{cases}$$

$$A_{c,\ell} = A'_{c,\ell} = \begin{cases} 0.05/300 \text{ mb}, & \text{for } 100 \text{ mb} \leq p_\ell < 400 \text{ mb cirrus} \\ 0.20/400 \text{ mb}, & \text{for } 400 \text{ mb} \leq p_\ell < 800 \text{ mb} \\ 0.30/200 \text{ mb}, & \text{for } 800 \text{ mb} \leq p_\ell \text{ and not cirrus} \end{cases}$$

where p_ℓ is the pressure of the upper surface of layer ℓ.

Appendix A13.1 Calculation of earth-sun distance and solar zenith angle

A13.1.1 Earth-sun distance

Although the earth's orbit around the sun is elliptic, the eccentricity of the earth's orbit is so small (e=0.01672) that the orbit is in fact very nearly circular. Therefore the earth-sun distance γ_E and the angular position of the sun $\omega(t)$ can be expressed as an asymptotic series in terms of mean angular position M(t) measured by a constant angular velocity with the periodicity of one year,

$$M(t) = \frac{2\pi}{T}(t - t_0), \tag{A13.1.1}$$

where T is 365 days, t_0 the time of perigee. The date of perigee adopted in the MRI•GCM-I is January 3.36 which is the mean date of perigee from 1950 through 1972. Therefore, M(t) is expressed as

$$M(t) = 0.0172142(t - 2.36), \tag{A13.1.2}$$

where t is the time in days counted from January 1. Then, from Kepler's second low

$$\gamma_E(t)/\bar{\gamma}_E = A_0 - A_1 \cos M - A_2 \cos 2M - A_3 \cos 3M - \cdots\cdots, \tag{A13.1.3}$$

$$\omega(t) = M + B_1 \sin M + B_2 \sin 2M + B_3 \sin 3M + \cdots\cdots,$$

where

$$A_0 = 1 + e^2 = 1.00027956,$$

$$A_1 = e - e^3 - e^5 - \cdots\cdots \approx 0.01671825,$$

$$A_2 = e^2 - e^4 - \cdots\cdots \approx 0.00013975,$$

$A_3 = e^3 - e^5 - \cdots\cdots$ ≈ 0.00000175,

$B_1 = 2e - e^3 + e^5 - \cdots\cdots$ ≈ 0.0334388,

$B_2 = e^2 - e^4 + \cdots\cdots$ ≈ 0.0003494,

$B_3 = e^3 - e^5 + \cdots\cdots$ ≈ 0.00000506,

and $\bar{\gamma}_E$ is one astronomical unit.

A13.1.2 Solar zenith angle

The cosine of the solar zenith angle is given by (13.45) ; the hour angle h is counted from the midday position and changes 15° per hour. Thus,

$$h(t) = \lambda + \frac{2\pi}{24}(t - t_G) \qquad \text{(A13.1.4)}$$

where λ is the longitude, t_G the midday time at Greenwich.

As for the solar declination δ, it is given by

$$\delta(t) = \sin^{-1}(\sin\epsilon \sin \ell) \qquad \text{(A13.1.5)}$$

where $\ell(t) = \omega(t) + \ell_0$ is ecliptic longitude of the sun, ℓ_0 the ecliptic longitude at perigee ($= -1.3550737$ rad or $-77.64°$), ϵ the inclinations of the earth's orbit ($= 23°27'$).

Appendix A13.2 Water vapor absorptivity function for the total solar spectrum, $A'_{H_2O}(X)$. E-5 means 10^{-5}

x ($g\ cm^{-2}$)	$A'_{H_2O}(x)$	$A_{H_2O}(X)=a+bx+cx^2$			$x=d+eA'_{H_2O}+fA'^2_{H_2O}$		
		a	b	c	d	e	f
1E-5	3.19E-4						
2	5.46						
3	7.43	8.61E-5	2.47E1	−9.92E4			
4	9.13						
5	1.07E-3				−1.17E-6	2.94E-2	1.172E1
6	1.22						
7	1.35						
8	1.48						
9	1.60	4.57E-4	1.37E1	−1.23E4			
1E-4	1.72						
2	2.69						
3	3.47						
4	4.12						
5	4.69						
6	5.22				−2.23E-6	3.20E-2	1.60E1
7	5.70	1.41E-3	7.52E0	−1.96E3			
8	6.15						
9	6.58						
1E-3	6.98						

Table (Continued)

x ($g\ cm^{-2}$)	$A'_{H_2O}(x)$	$A_{H_2O}(X)=a+bx+cx^2$			$x=d+eA'_{H_2O}+fA'^2_{H_2O}$		
		a	b	c	d	e	f
2E-3	1.01E-2	3.82E-3	3.47E0	−1.97E2	4.61E-4	−7.53E-2	2.22E1
3	1.25						
4	1.44						
5	1.61						
6	1.76						
7	1.90	1.06E-2	1.32E0	−1.62E1			
8	2.02						
9	2.13				1.32E-2	−1.20E0	4.69E1
1E-2	2.24						
2	3.03						
3	3.57						
4	3.99	2.25E-2	5.02E-1	−1.79E0			
5	4.32						
6	4.62				9.31E-2	−5.18E0	9.66E1
7	4.87						
8	5.10						
9	5.30						
1E-1	5.49						
2	6.80	4.23E-2	1.44E-1	−1.04E-1	6.29E-1	−2.33E1	2.49E2
3	7.64						
4	8.26						
5	8.75						
6	9.17						

Table (Continued)

x ($g\ cm^{-2}$)	$A'_{H_2O}(x)$	$A_{H_2O}(X)=a+bx+cx^2$			$x=d+eA'_{H_2O}+fA'^2_{H_2O}$		
		a	b	c	d	e	f
7E-1	9.53E-2	7.76E-2	2.82E-2	−3.14E-3	4.59E0	−1.12E2	7.45E2
8	9.85						
9	1.01E-1						
1E0	1.04						
2	1.22						
3	1.32				2.96E1	−5.12E2	2.35E3
4	1.41						
5	1.47	1.25E-1	−5.04E-3	−8.30E-5			
6	1.52						
7	1.57						
8	1.61				1.19E2	−1.64E3	5.90E3
9	1.64						
1E1	1.68						
2	1.89						
3	2.02				6.08E2	−6.70E3	1.90E4
4	2.11						
5	2.18						
6	2.24						
7	2.29	1.82E-1	8.01E-4	−2.00E-6			
8	2.33				2.60E3	−2.40E4	5.68E4
9	2.37						
1E2	2.40						
2	2.62						

Table (Continued)

x ($g\ cm^{-2}$)	$A'_{H_2O}(x)$	$A_{H_2O}(X)=a+bx+cx^2$			$x=d+eA'_{H_2O}+fA'^2_{H_2O}$		
		a	b	c	d	e	f
3E2	2.75E-1	2.41E-1	1.29E-4	−5.99E-8	1.30E4	−1.03E5	2.05E5
4	2.84						
4	2.91						
6	2.96						
7	3.00				6.57E4	−4.56E5	7.98E5
8	3.04						
9	3.08						
1E3	3.10						
2	3.29	2.94E-1	1.98E-5	−1.62E-9			
3	3.39				3.57E5	−2.22E6	3.46E6
4	3.46						
5	3.51						
6	3.55						
7	3.59	3.27E-1	5.98E-6	−2.02E-10	1.13E6	−6.58E6	9.62E6
8	3.61						
9	3.64						
1E4	3.66						

Appendix A13.3 Ozone absorptivity function for the total solar spectrum, $A'_{O_3}(X)$. E-5 means 10^{-5}

x (cm-NTP)	$A'_{O_3}(x)$	$A'_{O_3}(x)=a+bx+cx^2$		
		a	b	c
1E-5	1.48E-5	2.62E-7	1.47E0	−1.22E2
2	2.95			
3	4.42			
4	5.89			
5	7.35			
6	8.82			
7	1.03E-4			
8	1.17			
9	1.32			
1E-4	1.46			
2	2.90			
3	4.31			
4	5.70			
5	7.06			
6	8.39			
7	9.71			
8	1.10E-3			
9	1.23			
1E-3	1.35			
2	2.48	1.82E-4	1.25E0	−5.79E1
3	3.44			
4	4.26			
5	4.97			
6	5.59			
7	6.14			
8	6.63	3.24E-3	4.74E-1	−6.30E0
9	7.06			
1E-2	7.46			
2	1.01E-2			
3	1.18			
4	1.31	8.76E-3	1.16E-1	−2.26E-1
5	1.42			
6	1.51			
7	1.59			
8	1.66			
9	1.73			
1E-1	1.80E-2			

Table (Continued)

x (cm-NTP)	$A'_{O_3}(x)$	$A'_{O_3}(x)=a+bx+cx^2$		
		a	b	c
2E-1	2.30E-2			
3	2.70			
4	3.05			
5	3.37			
6	3.68	1.54E-2	4.08E-2	−8.51E-3
7	3.97			
8	4.25			
9	4.52			
1E0	4.78			
2	7.15			
3	9.21			
4	1.11E-1			
5	1.27	2.51E-2	2.44E-2	−7.83E-4
6	1.43			
7	1.57			
8	1.70			
9	1.82			
1E1	1.93			
2	2.70	7.85E-2	1.32E-2	−1.79E-4
3	3.12			